J. Phys.: Condens. Matter **11** (1999) 9365–9385. Printed in the UK PII: S0953-8984(99)05098-5

Growth of thin films

E Bauer

Department of Physics and Astronomy, Arizona State University, Tempe, AZ 85287-1504, USA

Received 10 June 1999

Abstract. The results of epitaxial growth studies of ferromagnetic metals for a selected class of nonmagnetic substrates is reviewed. The reverse sequence is also discussed for some systems of importance in double layer and sandwich studies. The interrelation between film structure and magnetic properties is pointed out for several examples.

1. Introduction

The rapid evolution of magnetic thin film sensors and memories during the past decade has not only led to an explosive growth of the literature on magnetic properties of thin films but to a similar development of studies of the growth of these films. This is in part due to the increasing number of experimental techniques suitable for growth studies and in part due to the recognition that the magnetic properties of the films depend strongly on the film structure which is largely determined by the growth. This article can, therefore, cover only a small fraction of the work in this field. It will not discuss the practical aspects of thin magnetic films. They can be found, for example, in the proceedings of the conferences on magnetic recording media [1] and of other conferences on magnetism and magnetic materials. Likewise, films on amorphous substrates, polycrystalline, sputtered and electrolytically deposited films will not be included. This leaves epitaxial layers grown under ultrahigh vacuum (UHV) conditions of which only a few could be selected. For a more general discussion of metal epitaxy on metals the reader is referred to older reviews [2, 3] and monographs, in particular to the articles in [4] which cover the various processes involved in epitaxy.

The review is organized as follows. After a brief description of the experimental methods growth on densely packed surfaces, mainly bcc (110) and fcc (111) surfaces will be discussed. Growth on fcc (100) surfaces is treated jointly with growth on bcc (100) surfaces. Films on other surfaces such as bcc (111), bcc (211), fcc (110) and hcp $(10\bar{1}0)$ as well as quasi-one-dimensional crystal growth on vicinal surfaces are touched only briefly. A discussion of the processes which allows us to tailor films such as nucleation control, use of misfit anisotropy, surfactants etc concludes this contribution.

2. Experimental methods

Of the many techniques in the arsenal of surface science the laterally averaging methods of reflection high energy electron diffraction (RHEED), low energy electron diffraction (LEED) and Auger electron spectroscopy (AES) have been most widely used in growth studies. Work function change ($\Delta\Phi$) measurements have also made valuable contributions, in particular in

0953-8984/99/489365+21$30.00

the monolayer range. More recently ultraviolet photoelectron spectroscopy (UPS) and x-ray photo-electron diffraction (XPD) have also been shown to be very useful. Although RHEED is still used for the determination of the film orientation, the specular beam intensity oscillations due to periodic atomic roughness changes has become its major application. Similarly, LEED not only gives the lateral periodicity and—with a dynamical intensity analysis—the atomic positions in the unit cell but in its SPALEED version—which has a high resolution in reciprocal space—also laterally averaged information on the surface topography. UPS allows us to monitor film growth via the sensitivity of the electronic structure to atomic environment up to several monolayers (ML) and XPD becomes an important tool for structural analysis beyond that thickness.

Our understanding of the growth of epitaxial films would be rudimentary were it not for the contributions which laterally resolving techniques, foremost scanning tunnelling microscopy (STM) and low energy electron microscopy (LEEM), have made. The initial problems of STM, thermal drift and shadowing by the tip, which made it impossible to monitor film growth, have been largely overcome so that growth processes can be studied now quasi-continuously by intermittent tip retraction. LEEM does not have these problems but at the expense of much lower lateral resolution than STM. However, many aspects of the growth do not need the resolution achievable with STM and the possibility to combine LEEM with LEED, spin-polarized LEEM (SPLEEM) and x-ray photo-emission electron microscopy (XPEEM) allows a comprehensive characterization of the topography, the crystal structure, the magnetic domain structure and the chemical composition of the film [5, 6]. The results reported below were obtained with a combination of several of these techniques. Others, of course, have contributed too but cannot be included here for lack of space.

3. Growth on densely packed surfaces

3.1. The bcc (110) surface

Although not close packed, these is the most densely packed surface of bcc metals and has long been a favourite substrate for epitaxy starting with the early studies of the growth of Cu on W(110) [7–9]. W(110) and Mo(110) substrates are so attractive because due to their high melting point they can be cleaned easily by flashing off deposited layers—with some precautions (see below)—so that they can be frequently reused. The (110) surfaces of the other bcc metals (Ta, Nb, Fe, Cr and V) are much harder to clean and have been used much less.

The surface energies of the ferromagnetic metals of interest here, Ni, Co and Fe are sufficiently lower than those of W and Mo so that Stranski–Krastanov growth is expected at elevated temperatures and quasi-Frank–van der Merwe growth at lower temperatures. On the basis of van der Merwe's structural phase diagram initially 1–2 pseudomorphic monolayers should form with the subsequent growth in the Nishiyama–Wassermann orientation of the fcc Ni and equivalent orientations of the hcp Co and the bcc Fe [10]. This growth sequence had already been observed earlier in the first AES/LEED/$\Delta\Phi$ study of Ni on W(110) [11] and was confirmed by the subsequent studies of this system [12–22] and of Ni on Mo(110) [23] with minor differences.

3.1.1. Ni on W(110) and Mo(110) The present state of understanding of the growth of Ni on W(110) and Mo(110) may be summarized as follows. At room temperature and below where nucleation rate is high and diffusion limited, two-dimensional (2D) pseudomorphic (ps) islands form initially with more or less dendritic shape. The 'dentricity' depends not only upon

deposition temperature and rate but also upon residual gas coadsorption, a problem encountered in all experiments in which the time between flashing the crystal and start of the deposition is long and/or the deposition is made cumulatively, for example in STM studies. Due to limited mobility, site blocking and possible Ehrlich–Schwoebel barriers at these temperatures, atoms landing on top of the islands cannot be incorporated at their edges and 'squeeze' into the island, transforming them into a close-packed (cp) structure with increasing coverage long before completion of the ps layer [24]. Alternatively the transition may occur spontaneously when two islands meet [11]. Only under very clean conditions and at elevated temperatures can the ps ML fully develop before the transition to the cp layer occurs. This is clearly evident in $\Delta\Phi$ measurements which are very sensitive to atomic roughness. Figure 1(a) shows in the upper part such $\Delta\Phi$ measurements for Ni on Mo(110) at temperatures at which kinetic limitations are negligible. Due to the loose packing in the ps ML Φ decreases initially nearly linear with coverage until the ps ML is completed and rises thereafter rapidly due to the formation of the cp layer. The subsequent change is slow because the 3D islands forming cover only a small fraction of the surface (600 K and 790 K) and because of alloying (880 K).

The AES measurements show only a small change of slope of the Ni signal at the ps $\rightarrow$ cp transition—which has been overlooked in less accurate work [13]—caused by changes in the electronic structure. These are clearly evident in the intensities of UPS spectra at energies which are particularly sensitive to structural changes as illustrated in figure 2 [17]. At a binding energy of 0.64 eV (b) the intensity suddenly increases strongly at the transition from ps to cp packing. For comparison also AES data are shown which were acquired at an emission angle (50°) more sensitive to structural changes than that used in figure 1(a) ($42 \pm 5^\circ$). Figure 2 also shows that the ps $\rightarrow$ cp transition occurs earlier at 300 K due to kinetic limitations. The effect of these limitations can be seen particularly well in figure 1(b) which shows the $\Delta\Phi$ change during heating after cumulative depositions of Ni on Mo(110) at 365 K. Above about 1/3 ps ML heating causes initially an increase of Φ due to the incorporation of atoms on top of the ps islands and resulting ps $\rightarrow$ cp transition followed by a strong decrease to the equilibrium ps structure. The decrease is strongest around 1 ps ML as one would expect. The additional subtle features in these curves are explained in [23].

Recent STM studies [20–22] are in apparent contradiction with the picture of the ps $\rightarrow$ cp tranistion derived from the laterally averaging studies discussed above. In the STM studies the cp (7×1) structure at 0.9 ML coverage could not be converted into the ps structure by annealing at 900 K. Future work has to show whether this is due to the higher step density on the surface used in the STM study or due to contamination. The second possibility is not unlikely as LEEM studies of the initial growth of Co on W(110)—which is very similar to that of Ni—have also shown holes in the ML similar to those observed in the STM work whenever the surface was contaminated.

The growth beyond the first ML depends strongly upon temperature. At 300 K RHEED specular beam intensity oscillations can be seen over about 10 ML, depending upon the angle of incidence. Growth in poor vacuum increases the range of the oscillations significantly and so does deposition in good vacuum at 100 K [12, 15, 16]. This does not necessarily mean monolayer-by-monolayer growth as frequently assumed but indicates only that the surface roughness varies periodically during growth. Nevertheless, quasi-Frank–van der Merwe growth occurs at least initially as the Auger data up to three ML show. In recent LEED work the film strain along the W[$1\bar{1}0$] direction could be observed up to 8 ML before the surface became rough [25]. Although the temperature at which alloying sets in has not been determined accurately, there is little doubt on the basis of AES and energy loss spectroscopy that alloying between Ni and Mo starts definitely below 900 K and levels off at the approximate composition NiMo at about 1100 K in layers more than 4 ML thick [23]. The situation on W

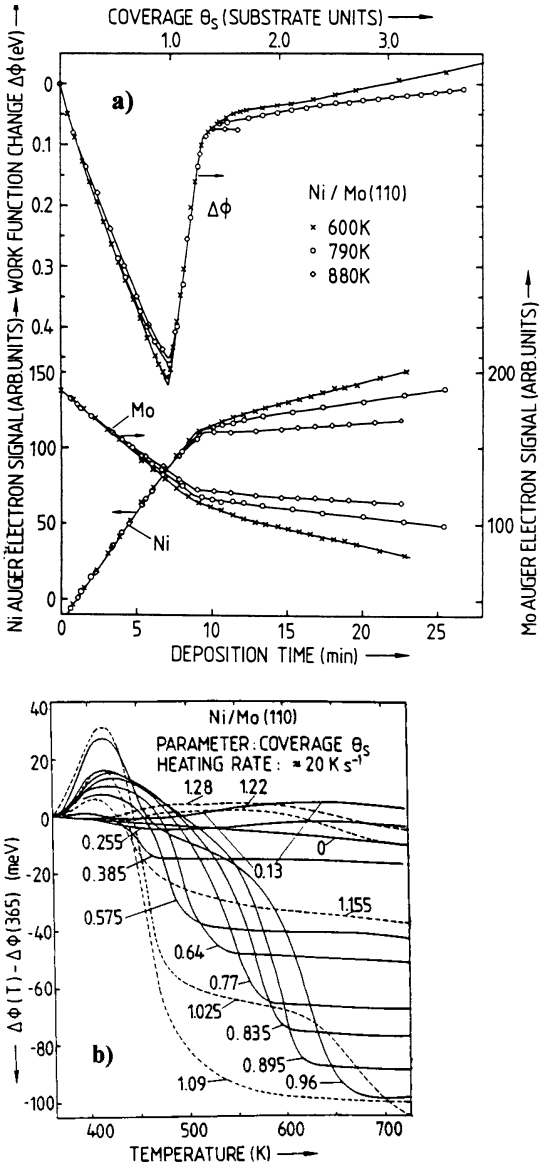

Figure 1. (a) Work function change $\Delta\Phi$, Ni and Mo Auger signals as a function of deposition time (bottom) and coverage (top) on Mo(110) at various temperatures, measured at temperature. (b) Work function change during heating after cumulative depositions at 365 K; coverage in ps units [23].

is believed to be similar [11]. It should be noted that the solubility of Ni in W and Mo is low but that W and Mo dissolve in Ni up to more than 20 at.%. Thus the Ni islands have to be large enough before alloying can start. No alloying occurs below 1 ML. The alloying problem is much clearer in Co films and will be discussed there in more detail. At lower temperatures the Ni layers grow in the Stranski–Krastanov mode as judged by the comparison with the AES and $\Delta\Phi$ data obtained at 300 K. For example, the slope of the AES signal in figure 1(a) beyond

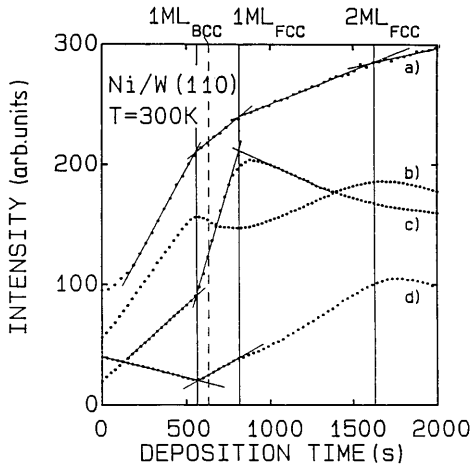

Figure 2. Ni AES and UPS signals as a function of deposition time (bottom) and coverage (top) on W(110). (a) Amplitude of differentiated $M_{2,3}M_{4,5}M_{4,5}$ (61 eV) Auger signal at a polar angle of 50° in the [001] azimuth. (b)–(d) UPS intensities in normal emission at 1.46 eV, 0.64 eV and 0.16 eV binding energy, respectively. The curves are shifted for clarity [17].

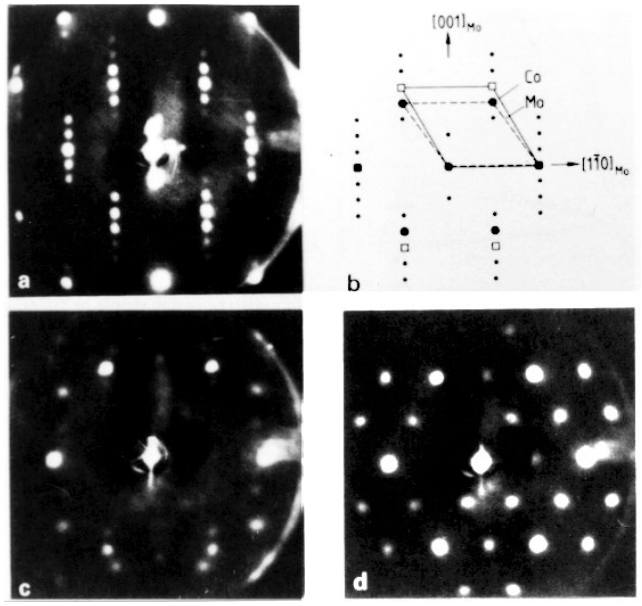

Figure 3. LEED patterns (a), (c), (d) and reciprocal lattice unit mesh (b) of pattern (a). (a), (b) (8 × 1), (b) complex and (c) p(2 × 2) structure. Energies 141 eV, 104 eV and 128 eV, respectively. (c) and (d) are from an alloy phase [23].

the first ML is significantly smaller at 600 K than at 300 K (not shown) and decreases further with increasing deposition temperature. More detailed data for Ni are not available.

3.1.2. Co on W(110) and Mo(110). The growth of Co on W(110) and Mo(110) has been studied in much more detail, though not with STM but with LEEM. First the results of the

DOCKET ALARM

Explore Litigation Insights

Docket Alarm provides insights to develop a more informed litigation strategy and the peace of mind of knowing you're on top of things.

Real-Time Litigation Alerts

Keep your litigation team up-to-date with **real-time alerts** and advanced team management tools built for the enterprise, all while greatly reducing PACER spend.

Our comprehensive service means we can handle Federal, State, and Administrative courts across the country.

Advanced Docket Research

With over 230 million records, Docket Alarm's cloud-native docket research platform finds what other services can't. Coverage includes Federal, State, plus PTAB, TTAB, ITC and NLRB decisions, all in one place.

Identify arguments that have been successful in the past with full text, pinpoint searching. Link to case law cited within any court document via Fastcase.

Analytics At Your Fingertips

Learn what happened the last time a particular judge, opposing counsel or company faced cases similar to yours.

Advanced out-of-the-box PTAB and TTAB analytics are always at your fingertips.

API

Docket Alarm offers a powerful API (application programming interface) to developers that want to integrate case filings into their apps.

LAW FIRMS
Build custom dashboards for your attorneys and clients with live data direct from the court.

Automate many repetitive legal tasks like conflict checks, document management, and marketing.

FINANCIAL INSTITUTIONS
Litigation and bankruptcy checks for companies and debtors.

E-DISCOVERY AND LEGAL VENDORS
Sync your system to PACER to automate legal marketing.